Performance Analysis of Doubly-Fed Induction Generator Connected to A Wind Turbine for Variable Wind Speed

Nagm Eldeen Abdo Mustafa Hassanain, Abdelaziz Y. M. Abbas, Omer Mohammed Elbabo Mohammed Hassan

Abstract — This paper presents the model and simulation of wind turbine drives doubly-fed induction generator, which feeds AC power to the utility grid. Two voltage source converters are used to extract maximum power from variable wind speed. The converters are connected back to back between the rotor terminals of the induction generator and utility grid via common dc link. The grid-side converter controls the power flow between the DC bus and the AC side. The rotor side converter control the output power generated. Matlab/Simulink software package is used to simulate the system. The results of two wind speed and two blade pitch angles are obtained and compared.

Index Terms —Induction generator, wind turbine, back to back converter, variable speed

——————————   ◆   ——————————

1 INTRODUCTION

Renewable energy such as solar, wind, and tidal currents of oceans is sustainable and environmental energy. Wind power generation has attracted great interest in recent years [1]. Large wind-plants compete with electric utilities in supply economical clean power in many parts of the world [2-4]. Most wind turbines use induction generators than the other type of generator. Because the rotor of induction generators does not require the exciter, brushes, and slip rings [5-7]. It has found that wound rotor induction generator is useful to apply in wind power generator. Wound rotor induction generators (WRIG) are provided with three phase windings on the rotor and on the stator. They supplied energy from both rotor and stator terminals. This is why they are called doubly fed induction generators (DFIGs) or double output induction generators (DOIGs). The WRIM is controlled by the machine-side converter to operate as a variable speed constant frequency generator whereas the grid-side converter operates as the power conditioner to control the active and reactive power of the rotor.. Both motor and generator operation modes are feasible, provided the power electronics converter that supplies the rotor circuits via slip-rings and brushes is capable of handling power in both directions.

As a generator, the WRIG provides constant or controlled voltage V_s and frequency f_1 through the stator, while the rotor is supplied through a static power converter at variable voltage V_r and frequency f_2. The rotor circuit can absorb or deliver electric power. The number of poles of both stator and rotor windings are the same.

In order to integrate the wind power into the utility there are many types of power electronics components are used in wind turbines [8-12]. Many control algorithms have been proposed and used for controlling the DFIG rotor- and grid-side converters for certain dynamic and transient performance achievements of DFIGs. Power generation over a range of speed means that increased energy capture is possible due to higher average aerodynamic efficiency [13]. Maximum power extract from variable speed wind turbine is the main challenge. In this paper the model of the wind turbine driven DFIG which feeds ac power to the utility grid is presented. The mathematical model of the whole system is built. The control algorithm is used to control the back to back converters, which are connected between the rotor terminals and utility grid via common dc link. The modeled system is simulated using Matlab/Simulink.

2 MATHEMATICAL MODEL OF DFIG FOR WIND TURBINE

The mathematical model of DFIG can be divided into:

2.1 Wind Turbine Model:

A wind turbine can be characterized by the non-dimensional curve of power coefficient C_p as a function of Tip-Speed Ratio (TSR) λ, where, λ is given in terms of rotor speed, ω_m (rad/s), wind speed, v(m/s), and rotor radius, R (m) as

$$\lambda = R\,\omega_m/v \quad \text{(rad)} \qquad (1)$$

Wind turbine power coefficient, C_p, depends on λ. If pitch angle, β, is incorporated, C_p becomes a function of λ and

$$C_p(\lambda,\beta) = 0.5176(116/\lambda_i - 0.4\beta - 5)e^{-21/\lambda_i} + 0.0068\lambda \qquad (2)$$

Where, $(1/\lambda_i) = (1/(\lambda + 0.08\beta)) - (0.035/(\beta^3 + 1))$

The power coefficient, C_p, curve is shown in Fig. 1 as a function of tip speed ratio and pitch angle. It can be

- *Nagm Eldeen Abdo Mustafa Hassanain. School of Electrical and Nuclear Engineering, College of Engineering, Sudan University, Sudan, E-mail:, nagemaldeenabdo@sustech.edu, nagmabdo1@gmail.com*
- *Abdelaziz Y. M. Abbas. School of Electrical and Nuclear Engineering, College of Engineering, Sudan University, Sudan, E-mail: abdelazizyousif@sustech.edu, abdelaziz.abbas67@gmail.com,*
- *Omer Mohammed Elbabo Mohammed Hassan, M.Sc. Student*

seen that as β increases, C_p decreases, thus the power produced by the WT is reduced. The mechanical output power of the wind turbine can be expressed as:

$$P_m = 0.5\,\rho\,A\,C_p\,(\lambda,\,\beta)\,v^3 \tag{3}$$

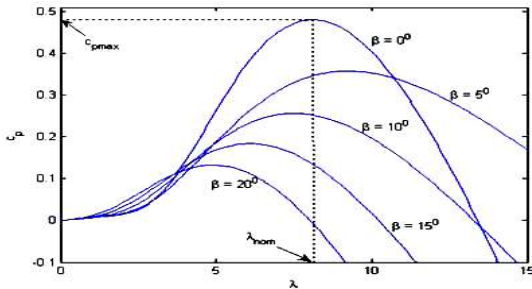Where, ρ is the air density (kg.m^{-3}) and A is the rotor rotational area, πR^2.

Fig. 1 Power coefficient as a function of tip speed ratio and pitch angle.

The output power for variable wind speed is shown in Fig. 2. From Fig. 2 it is found that when the wind speed is increased the maximum power extracted from the wind is increased for the same turbine speed.
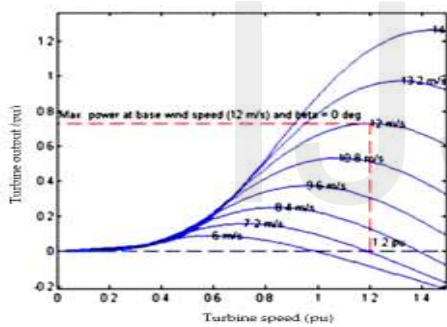

Fig. 2. Output power for variable wind speed

The equations of the wind turbine torque are.

$$T_m = p_m/\omega_m \tag{4}$$

$$(T_m - T_{shaft})/2H = d\omega t/dt \tag{5}$$

Where T_m is the mechanical torque, T_{shaft} is the shaft torque, H is the Inertia and p_m is the mechanical power.

2.2 Wound rotor induction generator model

In order to model the WRIG, Park's transformation model is used. Using standard motor principles, the mathematical representation of stator voltage, rotor voltage and the flux equations as per space vector theory can be described by :

$$V_{ds} = R_s i_{ds} \frac{d}{dt}\lambda_{ds} - \omega_s\lambda_{qs} \tag{6}$$

$$V_{qs} = R_s i_{qs} \frac{d}{dt}\lambda_{qs} - \omega_s\lambda_{ds} \tag{7}$$

$$V_{dr} = R_r i_{dr} \frac{d}{dt}\lambda_{dr} - \omega_r\lambda_{qr} \tag{8}$$

$$V_{qs} = R_r i_{qr} \frac{d}{dt}\lambda_{qr} - \omega_r\lambda_{dr} \tag{9}$$

$$\lambda_{ds} = (L_s + L_m)i_{sd} + L_m\,i_{rd} \tag{10}$$

$$\lambda_{qs} = (L_s + L_m)i_{sq} + L_m\,i_{rq} \tag{11}$$

$$\lambda_{dr} = (L_r + L_m)i_{rd} + L_m\,i_{sd} \tag{12}$$

$$\lambda_{qr} = (L_r + L_m)i_{rq} + L_m\,i_{sq} \tag{13}$$

Where, R_s, L_s, R_r, L_r are the resistances and leakage inductances of the IG stator and rotor windings respectively.

L_m is the mutual inductance, V_{qs}, V_{ds}, V_{qr}, V_{dr}, i_{sd}, i_{sq}, i_{rd}, i_{rq}, λ_{qr}, λ_{dr}, λ_{qs}, λ_{ds} are the d and q components of the space vectors of stator and rotor voltages, currents and fluxes linkage, ω_r and ω_s are the angular frequencies of stator and rotor currents respectively. In steady-state condition the above equations are given by the set of following equations [1].

$$V_{ds} = R_s i_{ds} - \omega_s\,[(L_s + L_m)i_{sq} + L_m\,i_{rq}] \tag{14}$$

$$V_{qs} = R_s i_{qs} + \omega_s\,[(L_s + L_m)i_{sd} + L_m\,i_{rd}] \tag{15}$$

$$V_{dr} = R_r i_{dr} - \omega_s\,[(L_r + L_m)i_{rq} + L_m\,i_{sq}] \tag{16}$$

$$V_{rq} = R_r i_{rq} + \omega_s\,[(L_r + L_m)i_{rd} + L_m\,i_{sd}] \tag{17}$$

The electromagnetic torque is

$$T_{em} = \lambda_{ds} i_{qs} - \lambda_{qs} i_{ds} \tag{18}$$

2.3 Back to back converter model

The AC/DC/AC converter is shown in Fig. 3. It is basically a PWM converter which uses sinusoidal PWM technique to reduce the harmonics present in the DFIG system. Wound rotor induction machine with its stator windings directly connected to the grid and its rotor windings connected to the grid through an AC/DC/AC converter. This kind of machine has fed the grid from both the rotor and stator sides. The converters are built by two self-commutated PWM converters, a rotor-side converter and a grid-side converter, with an intermediate DC voltage link. By controlling the converters on both sides, the DFIG characteristics can be adjusted so as to achieve maximum of effective power conversion or capturing capability for a wind turbine and to control its power generation with less voltage/power fluctuation [14-16].

The rotor-side converter controls the active and reactive power of the DFIG independently, and the grid-side converter controls DC-link capacitor voltage in a set value and maintains the converter operation with a desired power factor [5].
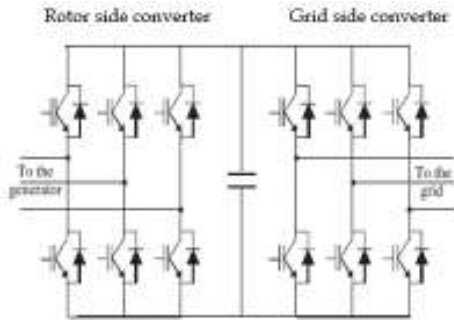
Fig. 3. Back to back converter

Fig. 4. Turbine power characteristic

A. Control model of rotor side converter

The rotor-side converter is used to control the wind turbine output power and the voltage measured at the grid terminals. The power is controlled using power-speed characteristic, named tracking characteristic. This tracking characteristic is shown in Fig. 4. The tracking characteristic is defined by four points: A, B, C and D. From zero speed to speed of point A the reference power is zero. Between point A and point B the tracking characteristic is a straight line. Between point B and point C the tracking characteristic is the locus of the maximum power of the turbine (maxima of the turbine power vs turbine speed curves). The tracking characteristic is a straight line from point C and point D. The power at point D is one. The actual speed of the turbine ω_r is measured and the corresponding mechanical power of the tracking characteristic is used as the reference power for the power control loop. For the rotor-side controller the *d-axis* of the rotating reference frame is used and aligned with air-gap flux. The actual electrical output power, measured at the grid terminals of the wind turbine, is added to the total power losses (mechanical and electrical) and is compared with the reference power obtained from the tracking characteristic. A Proportional-Integral (PI) regulator is used to reduce the power error to zero. The output of this regulator is the reference rotor current I_{qr_ref} that must be injected in the rotor by converter. This current component produces the electromagnetic torque T_{em}. The actual I_{qr} component is compared to I_{qr_ref} and the error is reduced to zero by a current regulator (PI). The output of this current controller is the voltage V_{qr} generated by rotor side converter. The current regulator is assisted by feed forward terms which predict V_{qr}. The voltage at grid terminals is controlled by the reactive power generated or absorbed by the converter. The reactive power is exchanged between rotor side converter and the grid, through the generator. In the exchange process the generator absorbs reactive power to supply its mutual and leakage inductances. The excess of reactive power is sent to the grid or to rotor side converter [6].
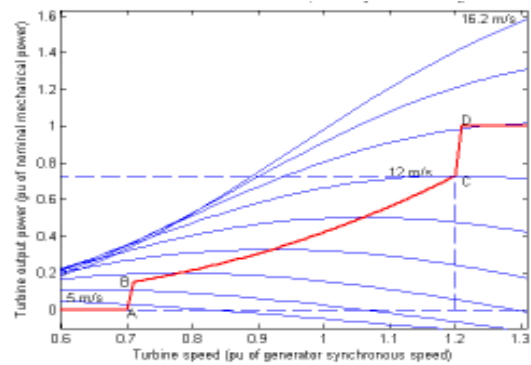
B. Grid side converter control system:

The Grid side converter is used to regulate the voltage of the DC bus capacitor. This controller consists of:

- A measurement system measuring the *d* and components of AC currents to be controlled as well as the DC voltage V_{dc}.
- An outer regulation loop consisting of a DC voltage regulator.
- An inner current regulation loop consisting of a current regulator.

The current regulatory controls the magnitude and phase of the voltage generated by converter grid side converter (V_{gc}) from the I_{dgcref} produced by the DC voltage regulator and specified I_{q_ref} reference. The current regulator is assisted by feed forward terms which predict the grid side converter output voltage [5].

C. DC link

The dc-link voltage must be higher than the peak main voltage; the dc-link voltage is regulated by controlling the power flow to the ac grid [7].

D. VSC with DC link Model

The model of rotor side converter and grid side converter are shown in Fig. s 5 and 6 respectively. The DFIG uses a pair of VSCs connected back-to-back through a DC link. The rotor-side VSC is connected to the WRIG rotor winding and the grid-side VSC is connected through a transformer to the stator terminals. In this model of the rotor-side VSC, when viewed from the AC side, it is represented by a controlled voltage source V_{rabc}.

$$V_{rabc} = \left| v_{rabc} \right| (\cos \delta_{rabc+} j \sin \delta_{rabc}) \qquad (19)$$

In this model of the grid-side VSC, when viewed from the AC side, it is represented by a controlled voltage source V_{gabc}.

$$V_{gabc} = \left| v_{gabc} \right| (\cos \delta_{gabc+} j \sin \delta_{gabc}) \qquad (20)$$

In the VSC models,δ_{rab},δ_{gabc} are the phase angles of the fundamental components of the pulse width modulation (PWM) waveforms. V_{rabc} and V_{gabc} are controlled by the modulation indices (M_g and M_r) of the PWMs. In both VSCs, M_g and M_r are defined as:

$$M_g = K_g \frac{|V_{gabc}|}{V_{dc}} \qquad (21)$$

$$M_r = K_r \frac{|V_{rabc}|}{V_{dc}} \qquad (22)$$
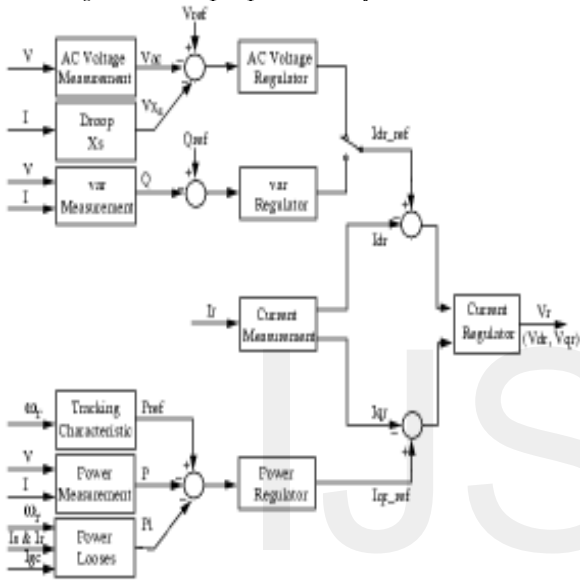
Where, k_g and k_r are proportionality constants [8].

Fig. 5. Rotor side converter control model.
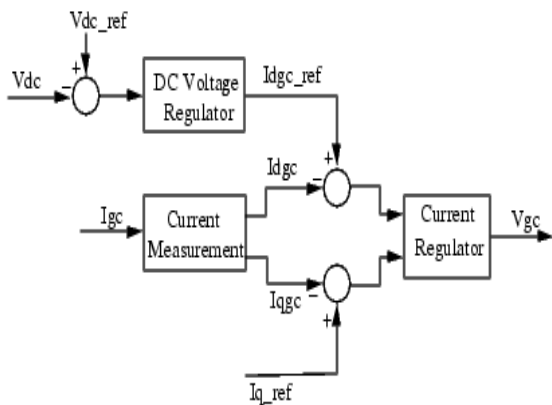
Fig. 6. Grid side converter control model.

3 RESULYS AND DISCUSSIONS

In this paper, a wind farm 9MW consisting of six 1.5MW wind turbines is used to simulate the complete system. The doubly-fed induction generators (DFIG)

consist of a wound rotor and AC/DC/AC IGBT-based PWM converter is connected directly to the 60 Hz, 25kV distribution system exports power to a 120kV grid through a 35km while the rotor is fed at variable frequency through the AC/DC/AC converter. The DFIG technology allows extracting maximum energy from the wind for low wind speeds by optimizing the turbine speed and minimizing mechanical stresses on the turbine during gusts of the wind.

This model is simulated using Matlab/Simulink program and the results are obtained. The simulation for two different wind speeds and two pitch angle is presented. The results are compared and discussed.

3.1 Simulation at wind speed 15 m/s

Fig. 7 shows the result of rotor speed, when the wind speed is 15m/s. Fig. 7 shows that at t=0 the rotor speed is 1.2 pu, power is 9 MW and pitch is 8.72. Due to acceleration of wind the rotor speed increasing smoothly at t = 0.03s and continuous increasing until it reach its maximum at t=0.134s, after that rotor speed starting decreases due to operation of control system. From Fig. 7 it is found that the maximum value of rotor speed is (1.2163 pu) at t = 0.134s and the minimum value of rotor speed is (1.1989pu) occurs at t = 0.0348 s.
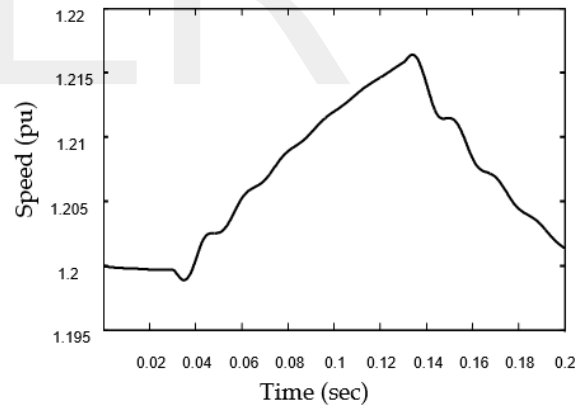

Fig. 7. Rotor speed curve at wind speed 15m/s

Fig. 8 shows the result of output power when the wind speed is 15m/s. The power starting increasing smoothly at t = 0.03s. As a result of acceleration of the rotor, it is found that the electro motive force decreases and then reduces the torque and thus power value.

From Fig. 8 it is observed that the power decreases smoothly at t = 0.035s. The power is again start increasing at t = 0.131s, due to rotor speed reduction. Also it is found that the maximum power (12.19 MW), and the minimum power (5.223 MW), occurs at t = 0.1533 s and t = 0.0532 s respectively.
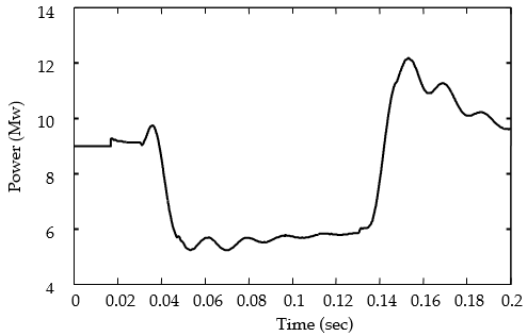
Fig. 8. Power curve at wind speed 15m/s

Fig. 9 shows the result of pitch angle, when the wind speed is 15m/s. the pitch curve which start increases smoothly at t = 0.02s, after that decreases smoothly at t = 0.043s, and again start increases at t=0.08. From Fig. 9 the maximum value of pitch angle (9.38) and the minimum value of pitch angle (8.52) occurs at t = 0.182 s and t = 0.082s respectively. it is noticed that the Pitch angle automatically changes with changes in rotor speed.
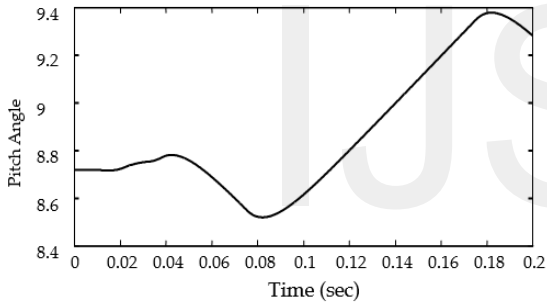

Fig. 9. Pitch angle curve at wind speed 15m/s

3.2 Simulation at wind speed 12 m/s

Fig. 10 shows the result of rotor speed, when the wind speed is 12m/s. At starting the rotor speed is 1.2 pu, the power is 9 MW and the pitch angle is 8.72. Due to wind acceleration the rotor speed curve increases smoothly at t=0.035s and continuous increasing until it reach its maximum at t=0.134s, then the rotor speed start decreases as a result of control system operation.

It is found that the maximum value of rotor speed is (1.214 pu) and the minimum value of rotor speed is (1.1955 pu) occurs at t = 0.134s and t = 0.2s respectively as shown in Fig. 10.
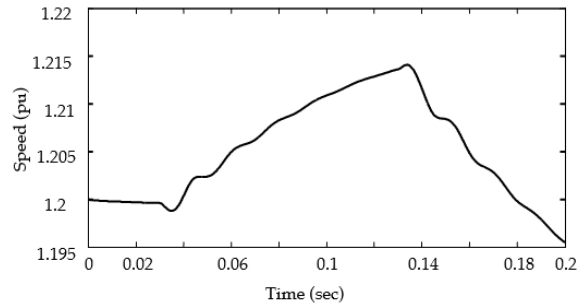

Fig. 10. Rotor speed curve at wind speed 12m/s

Fig. 11 shows the result of output power, when the wind speed is 12m/s. The power increases smoothly at t = 0.03s. As a result of rotor acceleration it is found that electro motive force decreases and then reduces the torque and thus the power value.

It can be observed that the power curve in Fig. 11 is decrease smoothly at t = .035s, and it start again to increase at t = 0.13s due to reduction in rotor speed. Also, the maximum power (12.12 Mw), and the minimum power (5.21 Mw), occurs at t = 0.1532 s and t = 0.0532 s respectively.
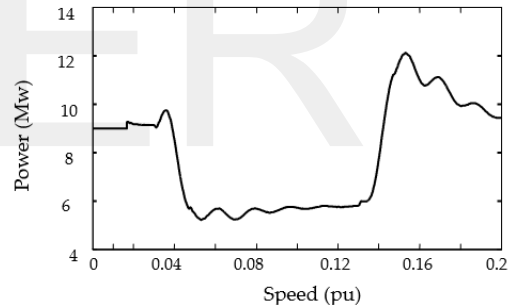

Fig. 11. Power curve at wind speed 12m/s

The result of pitch angle when the wind speed is 15m/s is depicted in Fig. 12 the pitch angle curve which start increases smoothly at t = 0.02 s, and then decreases smoothly at t = 0.0425 s, and at t = 0.088 again start increases. The maximum value of pitch angle (9.154) and the minimum value of pitch angle (8.503) occurs at t=0.172s and t = 0.0874s respectively as illustrated in Fig. 12.

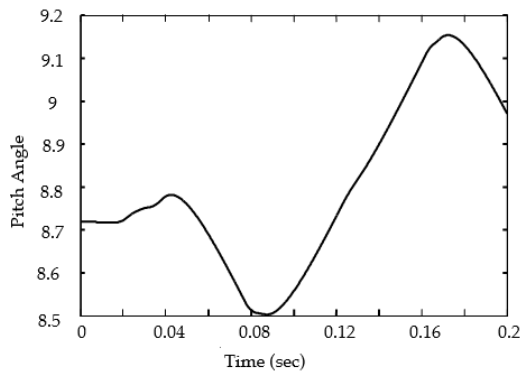It can be noted that the pitch angle automatically changes with changes in rotor speed.

Fig. 12. Pitch angle curve at wind speed 12m/s

3.3 Comparison between the two wind speeds results

Table 1 show the results of the simulation when the wind speed is 15 m/s and 12 m/s. When the wind speed increases and the back to back converters are used the output power of the generator is increased. Also, the value of pitch angle automatically is change with the wind speed to protection the system from strong wind and also to extract the maximum possible power from slow wind as illustrated in Table 1.

TABLE 1
COMPARISON BETWEEN THE TWO WIND SPEED RESULTS

Wind speed (m/s)	Max power (Mw)	Max rotor speed (pu)	Max pitch angle
15	12.19	1.2163	9.83
12	12.12	1.214	9.154

3.4 Simulation at constant wind speed and changing pitch angle

Two pitch angles is used in this simulation to extract the maximum power from wind turbine.

A. Simulation at maximum pitch angle =8°

Fig. 13 shows the result of rotor speed when the wind speed is 12m/s and maximum pitch angle is 8. At starting the rotor speed is 1.2 pu, the power is 9 MW and pitch angle is 8.72. Due to acceleration of rotor speed the power start increases smoothly at t=0.035s and continuous increasing until it reach its maximum at t=0.134s, then the rotor speed start decreases due to operation of control system.

The maximum value of rotor speed is (1.2142pu) and the minimum value of rotor speed is (1.196pu) occurs at t=0.134s and t = 0.2 s respectively as shown in Fig. 13.
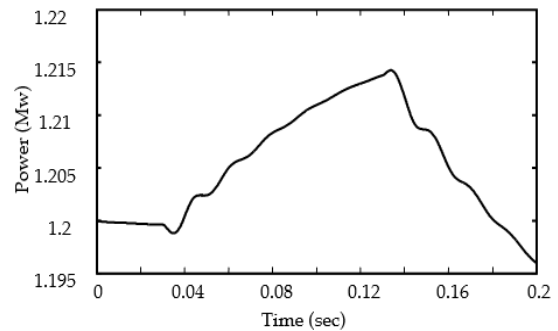

Fig. 13 Rotor Speed curve at wind speed 12m/s and pitch angle 8°

The result of output power, when the wind speed is 12m/s and maximum pitch angle=8 as depicted in Fig. 14. The power start increases smoothly at t=0312s. As a result of acceleration of the rotor the electro motive force decreases and then reduces the torque and thus the power value. It can be observed that the power is decrease smoothly at t=0.0362s and again start increases at t=0.13s as shown in Fig. 14, due to reduction in the rotor speed. The maximum power (12.141 MW), and the minimum power (5.21 MW), occurs at t=0.1533s. and t=0.0532s respectively.
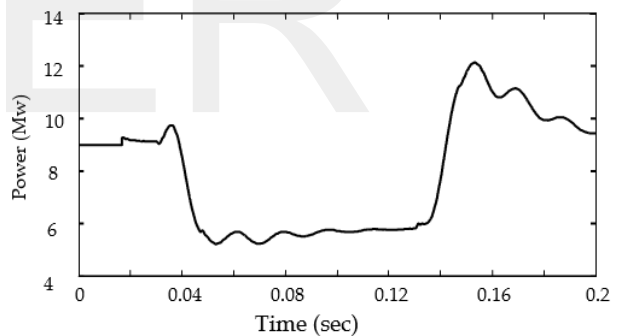

Fig. 14 Power curve at wind speed 12m/s and pitch angle 8°

Fig. 15 shows the result of pitch angle when the wind speed is 12m/s and the maximum pitch angle is 8°. This curve is immediately start decreases and continuous decreasing until it reach its minimum value of pitch angle (7.705°) at t=0.082s. Then the pitch angle start increases smoothly until it reach its constant value of pitch angle (8°) at t =0.016 s.
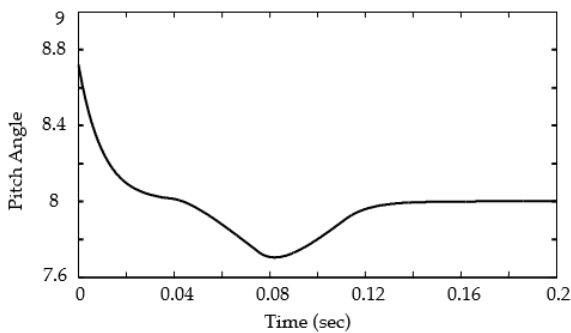
Fig.   15 Pitch angle curve at wind speed 12m/s and pitch angle 8°

B. Simulation at maximum pitch angle (5°)

Fig.   16 and Table 2 show the result of rotor speed, when the wind speed is 12m/s and maximum pitch angle is 5°. At starting the rotor speed is 1.2 pu, the power is 9 MW and the pitch angle is 8.72°. Due to acceleration of the rotor speed increases smoothly at t=0.035s and continuous increasing until it reach its maximum value at t=0.1342s, then the rotor speed start decreases because of the operation of the control system.

The maximum value of rotor speed is (1.2149 pu) at t=0.134s and the minimum value of rotor speed is (1.1976 pu) occur at t=0.2s as illustrated in Fig. 16.
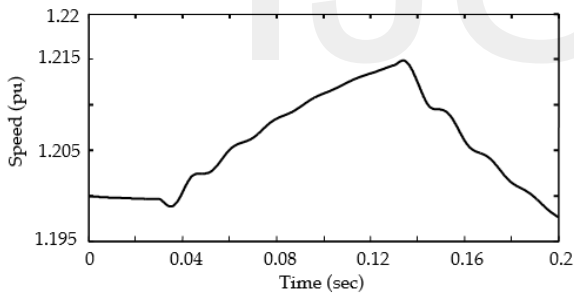

Fig. 16 Rotor Speed curve at wind speed 12m/s and pitch angle 5°

The result of output power when the speed of wind is 12m/s and maximum pitch angle is 5° is depicted in Fig. 17. The power start increases smoothly at t=0.0312s. The electro motive force decreases and then reduces the torque and thus the power value as a result of rotor acceleration.

It can be observed that the output power decreases smoothly at t=0.0362s and at t = 0.13 s the power again start increases due to the reduction in rotor speed as shown in Fig. 17. Also, it is found that the maximum power (12.151 MW) and the minimum power (5.203 MW) occurs at t=0.1533sand t=0.0534s respectively.
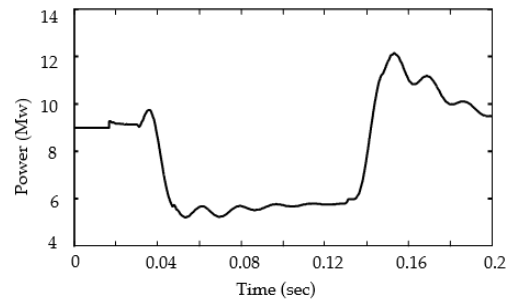

Fig. 17 Power curve at wind speed 12m/s and pitch angle 5°

Fig. 18 shows the result of the pitch angle, when the wind speed is 12m/s and the maximum pitch angle is 5°. This curve is immediately start decrease and continuous decreasing until it reach its minimum value of pitch angle (4.709°) at t=0.0819s. Then the pitch angle start increases smoothly until it reach its constant value of pitch angle (5°) at t=0.014s.
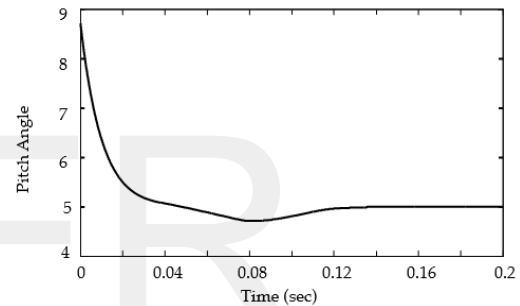

Fig. 18 Pitch angle curve at wind speed 12m/s and pitch angle 5°

C. Comparison between the two pitches angle results

Table 2 shows the results of the simulation for the two values of maximum pitch angle when the wind speed is 12m/s. When the values of pitch angle decrease the extracted power from wind increased as shown in Table 2. This result is identical to the power wind equation.

TABLE 2
COMPARISON BETWEEN THE TWO PITCHES ANGLE VALUES

Max Pitch angle	Max power (Mw)	Max rotor speed (pu)
8	12.141	1.2142
5	12.151	1.2149

4 CONCLUSIONS

This paper is presented the models and simulation of wind turbine driven doubly-fed induction generator using back to back converters which feeds power to the utility grid. The system model of a wind farm (9MW) consisting of six 1.5MW wind turbines has been presented. The model has simulated using Matlab/Simulink software. The results of the model

illustrated that the maximum extract possible output power from variable wind can be achieved by controlling the back to back converters system. The pitch angle controller is used to protect the system from strong wind and also to extract the maximum possible power from slow wind. The results are compared for two wind speed, 15m/s and 12m/s and two pitch angles 8° and 5°. The results show that the maximum output power is increased when the wind speed is 15m/s by 0.07MW more than the output power when wind speed is 12m/s. Also, the results show that when the maximum pitch angle is 5° and the wind speed is 12m/s the output power has increased 0.01MW more than the output power when maximum pitch angle is 8°. In this paper, it is found that the wind turbine connected to doubly Fed Induction Generator using back to back converters can extract more power from wind.

REFERENCES

[1] S. mazari, "Control Design and analysis of doubly fed induction generator in wind power application," Tuscaloosa, Alabama, Shukul mazari,2009.

[2] Mukund r. Patel, "*Wind and solar power system*," [2nd edition], CRC Press,2006.

[3] M. Stiebler, "Wind energy system for electric power generation,"Spring-Verlag Berlin Heidelberg, 2008.

[4] J. Zhang. Ming Cheng, Z. Chen, and X. Fu, "*Pitch angle control for variable speed wind turbines*,"DRPT2008, 6-9 April 2008, Nanjing China.

[5] A. Hemami, "Wind turbine technology," Cengage Learn, 2012.

[6] G. M. Master, "*Renewable and efficient power systems*," Stanford University, A John Wiley & sons,Inc., 2004.

[7] L. H. Hansen, L. Helle, F. Blaabjerg, E. Ritchie, S. Munk-Nielsen, H. Bindner, P. Sorensen and B. Bak-Jensen "Conceptual survey of generators and power electronics for wind turbines,"Riso-R-1205(EN),Pitney Bowes Management Services Denmark, December 2001.

[8] T. Ackerman, "Wind power in power system Edited," Royal institute of Technology Stockholm, Sweden, John willy &sons, Ltd., 2005.

[9] N. R. Bhasme,Dr. W. Z. Gandhare, "Power converter for grid integration of wind power system," Maharashtra-India,Vol.2. Issue4, July-August 2012.

[10] Khomfoi, L. M. Tolbert, "Multilevel power converter," Power Electronics Handbook, 3rd Edition. 2010

[11] A. Petersson, "Analysis Modeling and control Double fed Induction generators for wind turbines," Andreas Petersson, 2005.

[12] A. Kumhar Dadhania, "Modeling of double feed induction generator for distribution system power flow analysis," Ryerson University, Toronto, Ontario, Canada, Amit Kumar Dadhania, 2011.

[13] D. J. Atkinson, R. A. Lakin and R. Jones, "*A vector-controlled double-fed induction generator for a variable-speed wind turbine application*," Trans. Ins Mc Vol. 19, No.1, 1997.

[14] M. Pattnaik, "*Study of Doubly –Fed Induction generator for variable speed wind energy conversion systems*," Special Issue of International Journal of Power System Operation and Energy Management, ISSN (PRINT): 2231 – 4407, Volume -1, Issue-3.

[15] A. Kumar AG Rawal, B. Munshi, and S. Kayal, "Study of wind Turbine Driven DFIG using AC/DC/AC converter," Rourkela-769008, 2010.

[16] A. Carlsson, "The back to back Converter control and design," Reprocentralen, Lund, 22 May, 1998.